

## Atmospheric Tidal Variations within the ERICA Drifting-Buoy Data

ROBERT A. COHEN AND CARL W. KREITZBERG

*Department of Physics and Atmospheric Science, Drexel University, Philadelphia, Pennsylvania*

4 September 1991 and 18 December 1991

### ABSTRACT

The impact of atmospheric tides on surface pressure is studied by analyzing observations from the drifting-buoy network in the northwest Atlantic Ocean in winter 1988/89. These small, relatively inexpensive buoys, deployed for the Experiment on Rapidly Intensifying Cyclones over the Atlantic (ERICA), reported 10-min averages of air pressure, temperature, and sea surface temperature through satellites. Tidal oscillations are evident within the pressure variations and these tidal variations can be extracted and analyzed because they have a known constant period. The analyzed tides are compared with past observations and the similarities and differences are discussed. Many of the differences are attributed to the absence of local forcing in the homogeneous ocean environment, suggesting that the global-scale tide is being represented well. In this context, the observed variations agree well with what is expected, which demonstrates that the ability of the buoys to measure temporal changes is, on average, quite good. In addition, though the spatial gradients of tidal surface pressure variations at sea are negligible for most purposes, the magnitude of the temporal pressure variations are as large as  $1 \text{ mb } (3 \text{ h})^{-1}$ , which is significant compared to the  $3 \text{ mb } (3 \text{ h})^{-1}$  indicative of rapid storm development. The different treatment of tide-producing mechanisms in different numerical prediction models may also complicate inter-comparison of pressure changes over a few hours in global models versus regional models.

### 1. Introduction

A time trace of surface pressure will reveal small, 12-h (semidiurnal) oscillations embedded in the larger-scale, weather-dependent fluctuations (see Fig. 1). These oscillations are representative of atmospheric tides, so named because of their similarity with the tides in the ocean. In general, atmospheric tides only include oscillations that are global in scale (Chapman 1951). Periodic oscillations excited by local forcing (e.g., the sea breeze) are not usually considered tidal, although they are commonly referred to as nonmigrating tides (Tsuda and Kato 1989).

The data used in this study came from the ERICA (Experiment on Rapidly Intensifying Cyclones over the Atlantic) network of drifting buoys. These buoys were deployed as part of the field phase of ERICA, a program carried out during the winter (December–February) of 1988/89 to study the rapid intensification of storms at sea (Hartnett et al. 1989). Over the course of the ERICA field phase, 91 buoys operated in the northwest Atlantic Ocean (see Fig. 2), with lifetimes varying from 3 to 90 days. Observations of surface pressure, sea surface temperature, and air temperature were averaged over 10-min intervals and transmitted through the Argos system on polar-orbiting satellites at about 90-s intervals. After outliers were removed

(about one of every six observations were unusable because of transmission errors), corrections were made to compensate for known sensor and transmission-time problems. The buoy data were then interpolated to hourly values in universal time coordinated (UTC) via a third-order Bessel function fit and made available by the ERICA Data Center at Drexel University. For use in this tidal study, these hourly data were converted to local solar time (LST).

Although the resulting quality-controlled buoy data look very good, the sparsity of comparison observations over the ocean makes quality determinations difficult. Comparing the tidal oscillation as measured by the buoy data with past observations gives an indication of the buoy measurement system's ability to measure pressure changes.

A study of the tidal effects over the ocean is appropriate for other reasons also. While the oscillations are small in comparison to the amplitude of the weather variations (the semidiurnal oscillation in the ERICA region can have an amplitude of 1 mb over a period of 12 h and a wavelength of  $180^\circ$  longitude), the pressure tendency caused by the tidal variation becomes more important as the time scales of observations and forecasts grow shorter. Also, relative to land, the ocean surface is spatially homogeneous and less likely to undergo large temporal temperature changes (although the spatial gradients can be very large, especially near the Gulf Stream). This allows a determination of tidal pressure change that is less likely to be affected by local conditions.

Corresponding author address: Robert A. Cohen, Department of Physics and Atmospheric Science, Drexel University, Philadelphia, PA 19104.

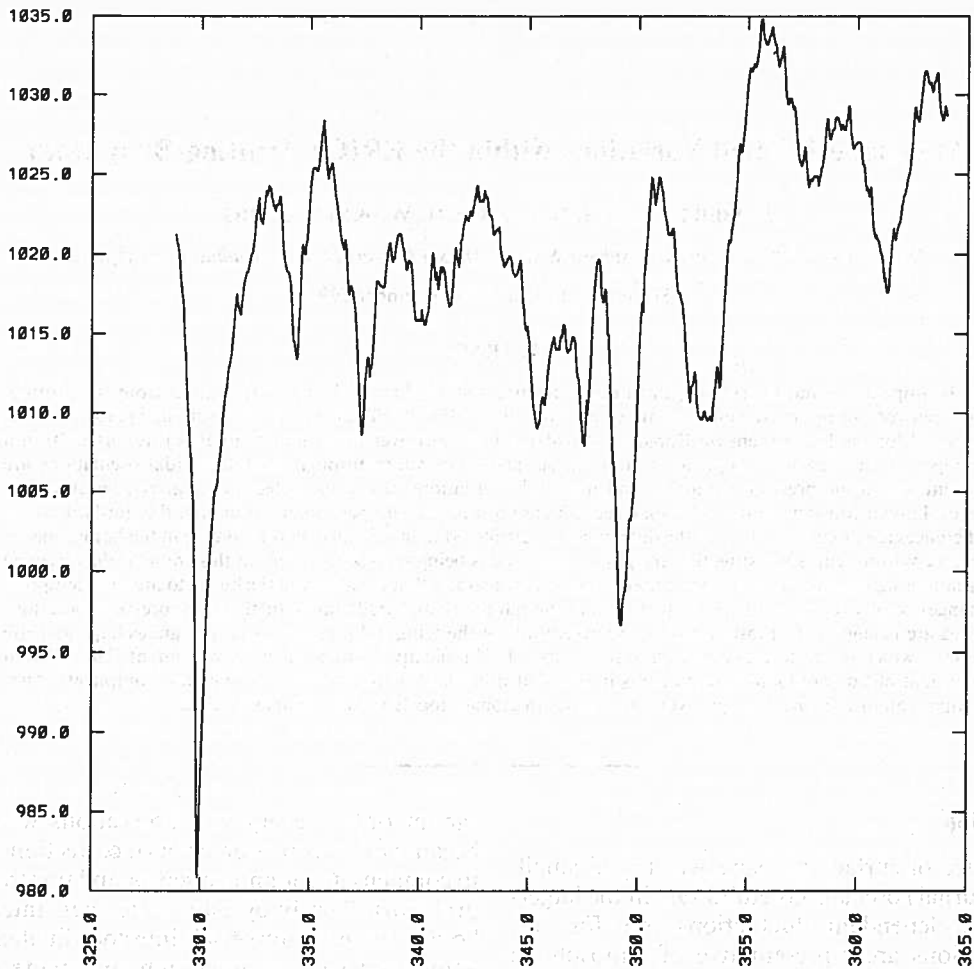


FIG. 1. Surface pressures (mb) versus Julian day (UTC; 1988) for ERICA buoy 11350. Day 330 corresponds to 25 November 1988.

## 2. Background

Tidal variations in the surface pressure trace have been documented since the early nineteenth century when Laplace observed them in barometric traces (Butler 1962). Since tides have a constant period, a tide can be produced whenever a force that has a constant period is present. In the case of the earth's oceans and atmosphere, periodic forcing comes from the sun (gravitational and thermal) and the moon (gravitational). Whereas the main reason for the oceanic tides is the difference in the moon's gravitational attraction from one area of the earth to another (the effect of the sun is about one-half that of the moon), the atmospheric tides, however, are due to daily thermal heating. The atmosphere absorbs solar radiation in three principal ways: directly via ozone absorption (20–70 km above the surface) and water vapor absorption (0–15 km) and indirectly through near-surface heating caused by eddy heat transfer with the earth's surface and latent heat release. Since the surface pressure is an integral

effect of the entire mass above the surface, the near-surface heating will contribute relatively little to the tidal oscillations of surface pressure, especially over the ocean where the surface temperature has a relatively small diurnal amplitude (see Fig. 4). Instead, it is mainly the absorption of solar radiation by ozone that produces the oscillation. Water vapor, being concentrated near the surface, contributes an effect about one-half that of ozone (Chapman and Lindzen 1970, p. 20).

Following this logic, one would expect a surface pressure oscillation that follows the temperature oscillation. A comparison between the daily averaged pressure and temperature traces (Fig. 3 and 4), however, reveals that there are two maxima of pressure during the day compared with only one for temperature. To understand why this is, one needs to understand the harmonic structure of the daily heating oscillation. The heating tends to be sinusoidal with a 24-h period during the day and zero during the night (Haurwitz 1964), so the heating curve (and similarly the temperature curve) over 24 h cannot be described with only one

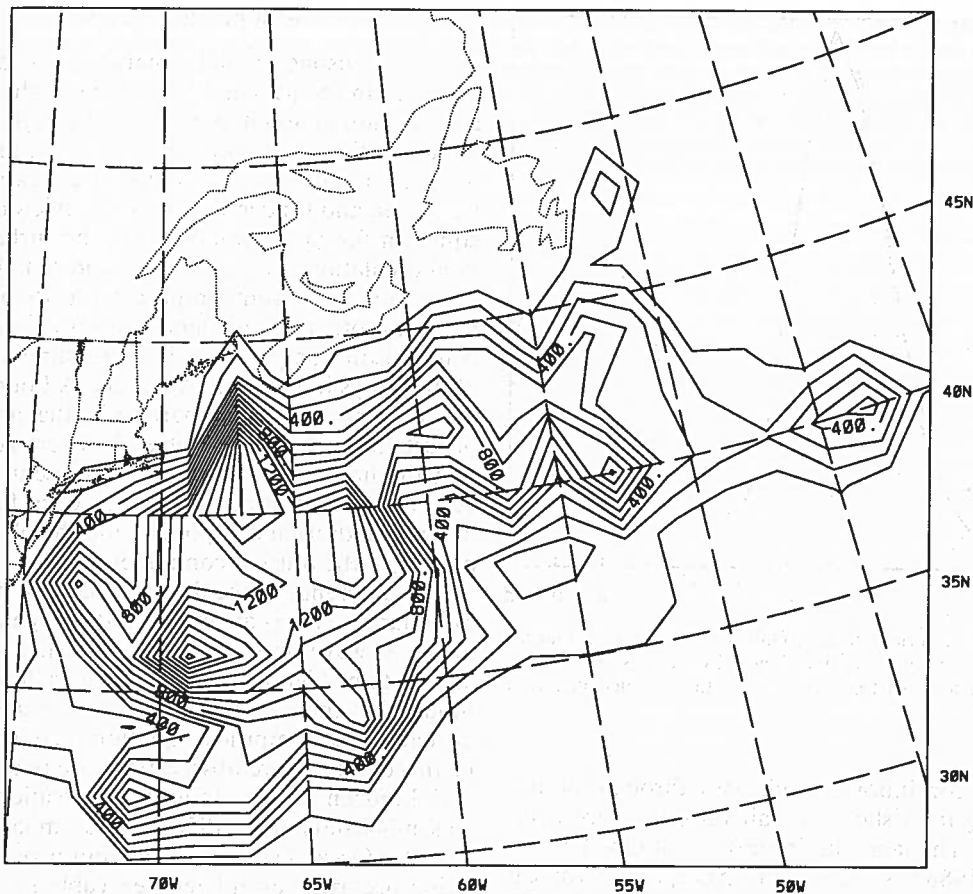


FIG. 2. Number of ERICA buoy hourly observations per  $2^\circ$  latitude-longitude square.

sine function of period one solar day. Indeed, a Fourier analysis of the temperature trace reveals that significant 12- and 8-h (or semidiurnal and terdiurnal) harmonics exist in addition to the main 24-h diurnal component (Table 1).

Furthermore, the atmosphere responds poorly to the diurnal harmonic (Chapman and Lindzen 1970) because the natural mode of the diurnal oscillation within the atmosphere has a vertical wavelength that is small in comparison to the forcing (50 km). This leads to interference. The semidiurnal mode, however, is large ( $\sim 200$  km; from Hamilton 1981). Subsequently, the semidiurnal component becomes the main component of the tidal oscillation of the surface pressure. Most of the actual diurnal component is caused by water vapor (Lindzen 1967) and near-surface heating (Zwiers and Hamilton 1986), and since these heat sources tend to vary with location, the diurnal oscillation is more susceptible to local influence (Kiser et al. 1963).

This process of the tidal surface pressure oscillation, as described above, has been pretty well understood since the early 1970s. Since that time, tidal research has shifted to the mesosphere and thermosphere (Forbes and Garrett 1979), where tides have a greater

influence on the circulation (Kahler 1989). Recently, however, some interest has been shown in the contribution of tides to mesoscale pressure tendencies (Mass et al. 1991), the contribution of localized heating to tides (Tsuda and Kato 1989), and the modeling of tides with general circulation models (Tokioka and Yagai 1987). Observations in the homogeneous ocean environment may be best for defining the zonally homogeneous or migrating tide isolated from any non-migrating tides excited by localized heating.

To simplify notation, tidal oscillations are frequently referred to as  $S_n$  or  $L_n$ , where  $S$  and  $L$  are used for oscillations caused by the sun and moon, respectively. The subscript  $n$  is the number of oscillations per solar day (24 h) or lunar day (24.84 h). For the oceans, the dominant pressure oscillation is  $L_2$ . For the atmosphere, the dominant pressure oscillation, measured on the earth's surface, is  $S_2$ .

### 3. Analysis of buoy data

Whereas previous studies of atmospheric tides over the ocean required ships for in situ observations, today measurement of the surface pressure over the ocean

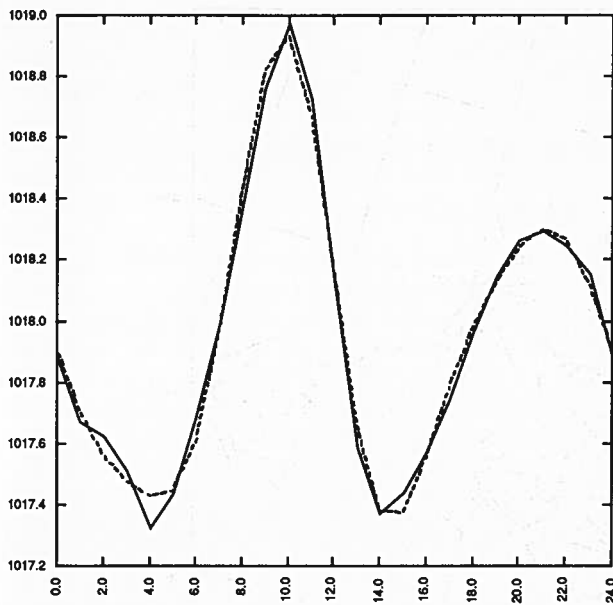


FIG. 3. Averaged surface pressure (mb) versus local solar hour for entire ERICA buoy set. Solid line shows observations; dashed line shows reconstructed trace from harmonics 0 to 4, as calculated from the observations.

can be done continuously and easily through the use of buoys. Figure 1 shows the air pressure trace from buoy 11350. The large dip in pressure at day 330 (25 November 1988) is due to the passage of Tropical Storm Keith. The dip in pressure at day 349 (14 December 1988) corresponds to the storm associated with ERICA intensive observation period (IOP) 2. Since buoy drift is only of order tens of kilometers per day, and since data are converted to local solar time, buoy-location errors have negligible impact on this analysis.

Subtracting a 12-h moving average from the trace reveals a semidiurnal oscillation with an amplitude of 0.5 mb (see Fig. 5). To get a better indication of these oscillations, a daily average on the pressures from the complete ERICA buoy set (see Fig. 2) is performed, which smooths any variations that have periods for which 24 h is not an integral multiple. The resultant graph (Fig. 3) shows a definite semidiurnal cycle. Together with the less-intense diurnal cycle, one gets a maximum at 1000 LST and a secondary maximum at 2100 LST. A Fourier analysis of this trace reveals a strong semidiurnal oscillation of amplitude 0.582 mb and a maximum at 0924 LST (see Table 1).

Before commenting further on the results, some discussion on the confidence of these values is appropriate. To gain a measure of error, data from the odd-numbered buoys were analyzed and compared with the data from the even-numbered buoys and the total set. The results (see Table 1) show that values such as the amplitude and phase of the semidiurnal oscillation would probably not change significantly with a larger sample size.

#### 4. Comparison with previous studies

This atmospheric tidal signature has been well documented in the past and has also been shown to have a maximum at about 1000 LST, although it is known to vary with season and latitude. As a comparison for the present study, four equations were extracted from Chapman and Lindzen's (1970) overview of tides, one equation for each component of the surface pressure tidal oscillation (i.e.,  $S_1$ ,  $S_2$ ,  $S_3$ , and  $S_4$ ). These equations, obtained from empirical fits to observations made by other researchers, were used to recreate a comparison tidal trace at the same time and location of the buoys in the ERICA dataset. A Fourier analysis of this composite reveals harmonics that are indicative of past observations (see Table 1). A comparison shows that the harmonics found in the present study agree very well with past observations, except for the phase of the semidiurnal component and the phase and amplitude of the diurnal component.

The difference in the diurnal phase, in particular, is quite large. This is attributed to the high dependence of the  $S_1$  wave on location. The diurnal oscillation is known to be highly influenced by local forcing such as mountains and coasts (Lindzen 1967), and so it is expected that the empirical equation used in Table 1 will be inaccurate where observations are poor (Chapman and Lindzen 1970). Indeed, observations made by Rosenthal and Baum (1956) from a similar area (North Atlantic Ocean) show the maximum of the  $S_1$  oscillation occurring even later (see Table 1).

These discrepancies in the diurnal oscillations of Table 1 are probably representative of nonmigrating

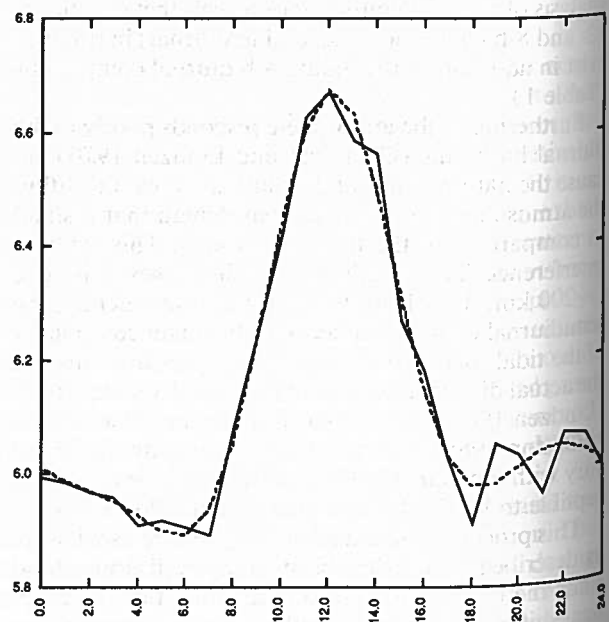


FIG. 4. Same as Fig. 3 except for air temperature ( $^{\circ}\text{C}$ ).

TABLE 1. Amplitudes ( $A_n$ ) and phases ( $\sigma_n$ , hour of maximum since local midnight) for selected datasets, where  $n$  = number of harmonic and  $(24/n)$  = period of oscillation. (a) Diurnal, semidiurnal, terdiurnal, and quaterdiurnal amplitudes ( $^{\circ}\text{C}$ ) and phases of air temperature from the complete ERICA buoy dataset. (b) Same as (a) except for surface pressure (mb). (c) Same as (b) except dataset consisted only of data from odd-numbered buoys or even-numbered buoys. (d) Same as (b) except dataset consisted of simulated pressures as calculated from a composite of equations found in Chapman and Lindzen (1970; pp. 34, 42, 43, and 44). (e) Same as (b) except for nine ships scattered across the North Atlantic for December, January, and February, as described in Rosenthal and Baum (1956).

Selected dataset	$A_1/\sigma_1$	$A_2/\sigma_2$	$A_3/\sigma_3$	$A_4/\sigma_4$	Number of observations
(a) ERICA temperatures	0.270/12.7	0.203/0.0	0.067/4.1	0.004/4.8	45 038
(b) ERICA pressures	0.139/11.5	0.582/9.4	0.203/1.9	0.092/4.1	45 038
(c) Odd-numbered buoys	0.196/10.8	0.600/9.3	0.192/1.9	0.102/4.1	20 812
Even-numbered buoys	0.101/12.8	0.570/9.4	0.213/1.9	0.087/4.0	24 226
(d) Simulated pressures	0.282/5.2	0.552/9.7	0.231/2.0	0.074/4.1	45 038
(e) Rosenthal and Baum (1956)	0.150/17.0	0.367/9.7	0.143/2.3	NA	NA

Note:  $S_n$  can be rewritten as  $A_n \cos[2\pi(t - \sigma_n)n/24]$ .

tides that are thought to be forced, in part, by the large diurnal heating over land (Tokioka and Yagai 1987). Thus, the smaller diurnal amplitude in the ERICA region may also be explained by the lack of a diurnal variation in air temperature over the ocean. Mass et

al. (1991) show that the diurnal amplitude varies somewhat proportionately to the surface air temperature. They found the average diurnal amplitude over the United States (in summer) to be 0.82 mb with an average temperature range of about  $13^{\circ}\text{C}$ . In compar-

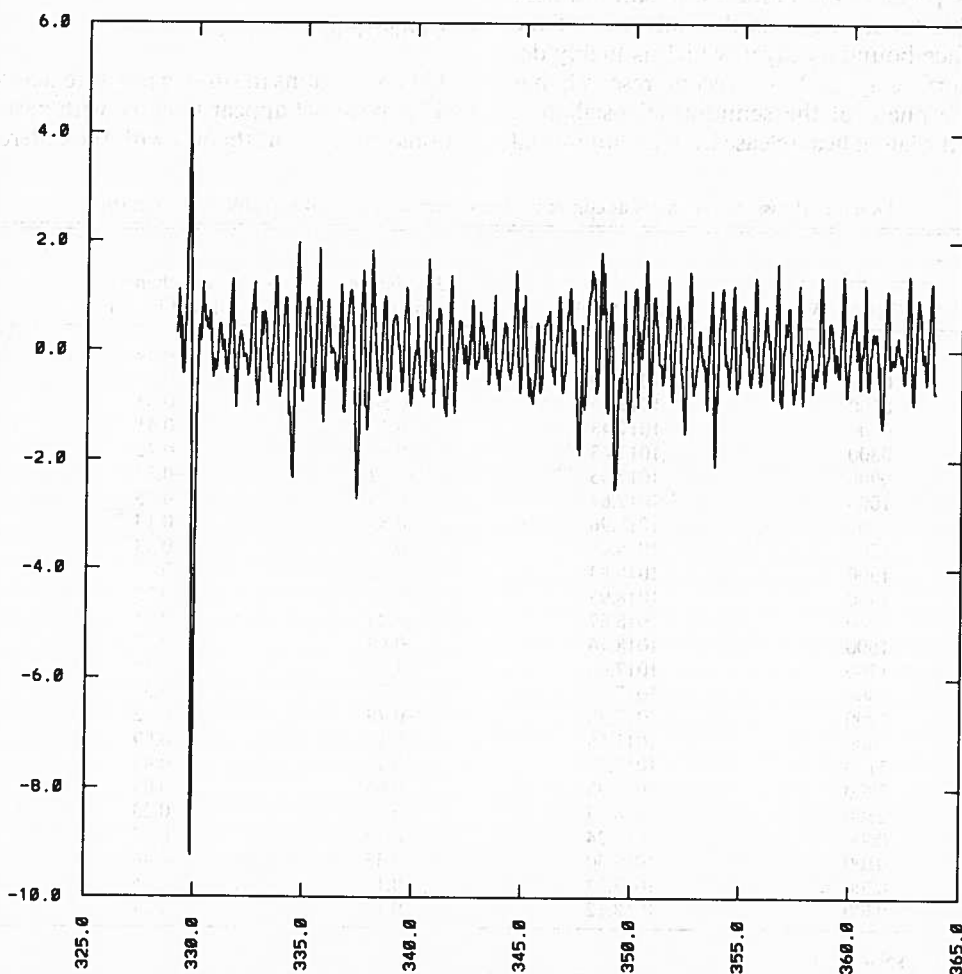


FIG. 5. Surface pressure deviations (mb) from 12-h mean versus Julian day (UTC; 1988) for ERICA buoy 11350.

ison, the average diurnal amplitude in the ERICA region (in winter) is 0.14 mb with an average temperature range of less than 1°C. It seems that the difference in local temperature range may be responsible for the difference in observed diurnal component.

Unlike the diurnal component, the difference in the phase of the semidiurnal component is small (9.4 versus 9.7 h). It is still, however, significant since the earlier phase appears consistently throughout the buoy dataset. This difference may be a result of seasonal variations. The empirical equation for  $S_2$  used to create the simulated observations did not include a seasonal variation. Figure 6 of Spar (1952) shows, however, that the maximum of the semidiurnal oscillation occurs before 0930 LST during winter and along the east coast of the United States. A closer look at the ERICA data reveals this seasonal variation in the semidiurnal phase with the phase varying among 0922 LST (December 1988), 0926 LST (January 1989), and 0930 LST (February 1989).

The earlier phase may also be closer to that predicted by theory. Chapman and Lindzen (1970) reported that inviscid theory predicts a semidiurnal maximum near 0900 LST. This theory neglects the influence of the turbulent surface boundary layer, which is highly dependent on surface type. More recent research has shown that the phase of the semidiurnal oscillation depends upon the latent heat release from a semidiurnal

oscillation in rainfall (Lindzen 1978; Hamilton 1981). It may be that the discrepancy in the semidiurnal phase is due to the difference in latent heat forcing over the ocean in winter. Another possible reason for discrepancies might be nonlinear interaction between the diurnal and semidiurnal tides (Teitelbaum et al. 1989) or the tides and planetary waves (Teitelbaum and Vial 1991), although research has been mainly limited to the mesosphere and thermosphere.

These discrepancies, however, are of little consequence when studying the pressure tendencies (i.e., change with time at one location) due to the tidal oscillations. Table 2 shows the 3-, 6-, and 12-h pressure tendencies as measured within the ERICA drifting-buoy data. It can be seen that the tidal oscillation causes pressure falls of 1.29 mb in the 3-h period ending at 1800 UTC (60°W), which is a significant portion of the 3 mb (3 h)<sup>-1</sup> pressure falls indicative of rapid storm development. In contrast, if one is concerned only with storm development over 12 h or more, tidal effects are minimal, as can be seen from the last column in Table 2.

## 5. Conclusions

Tidal variations in surface pressure derived from the ERICA buoy set appear to agree with past tidal observations and current theory, with the differences attrib-

TABLE 2. Pressure tendencies as computed from harmonics 1 to 4 in Table 1, dataset (b).

Time		Fitted (mb)	3-h change [mb (3 h) <sup>-1</sup> ]	6-h change [mb (3 h) <sup>-1</sup> ]	12-h change [mb (3 h) <sup>-1</sup> ]
(LST)	(UTC @ 60°W)				
0000	0400	1017.91	-0.40	-0.04	-0.06
0100	0500	1017.70	-0.56	-0.21	0.01
0200	0600	1017.56	-0.56	-0.34	0.05
0300	0700	1017.48	-0.43	-0.41	-0.03
0400	0800	1017.43	-0.28	-0.42	-0.03
0500	0900	1017.45	-0.12	-0.34	-0.08
0600	1000	1017.61	0.13	-0.15	-0.09
0700	1100	1017.96	0.53	0.13	-0.04
0800	1200	1018.43	0.98	0.43	0.05
0900	1300	1018.83	1.22	0.67	0.13
1000	1400	1018.93	0.97	0.75	0.17
1100	1500	1018.67	0.24	0.61	0.14
1200	1600	1018.16	-0.66	0.28	0.06
1300	1700	1017.66	-1.27	-0.15	-0.01
1400	1800	1017.38	-1.29	-0.53	-0.05
1500	1900	1017.38	-0.79	-0.72	-0.03
1600	2000	1017.56	-0.10	-0.69	0.03
1700	2100	1017.79	0.41	-0.44	0.08
1800	2200	1017.98	0.60	-0.09	0.09
1900	2300	1018.13	0.57	0.23	0.04
2000	0000	1018.24	0.46	0.43	-0.05
2100	0100	1018.30	0.33	0.46	-0.13
2200	0200	1018.27	0.14	0.36	-0.17
2300	0300	1018.12	-0.12	0.17	-0.14

Time (LST) = local solar time.

Time (UTC @ 60W) = UTC time that corresponds to "Time (LST)" at 60°W.

Fitted (mb) = value of the reconstructed Fourier fit using waves of period 6, 8, 12, and 24 h.

*n*-h change = change in the fitted curve over the past *n* hours, ending on that hour.

unable to the lack of nonmigrating tides in the homogeneous ocean environment, suggesting that the harmonic components within the buoy data represent the global-scale (migrating) tide rather well. These results also show that the buoy data, with many observations (over 45 000) over a relatively short time period [3 months, compared with 12 years of data by Kiser et al. (1963)] can accurately measure the tidal variations embedded within the larger day-to-day variations of pressure. The pressure tendencies measured by the buoys are apparently very good.

Traditionally, the tidal oscillations in the atmosphere are not considered when cyclonic-scale weather events are modeled. With mesoscale disturbances developing in 6 h [ERICA-type rapid intensification is defined in Hadlock and Kreitzberg (1988) as being  $10 \text{ mb (6 h)}^{-1}$  for at least 6 h], however, the tidal pressure tendencies on the order of  $1 \text{ mb (3 h)}^{-1}$  may be significant. Although any global circulation model that includes the daily absorption of solar radiation will produce the tidal motions (Kahler 1989), to our knowledge no study has been conducted of tidal variations in regional numerical weather prediction models. It is expected that the lateral boundary conditions and incomplete ozone definition in many regional models could eliminate tidal pressure oscillations. If this speculation is correct, intercomparison of global and regional model forecasts of pressure changes over a few hours could be more difficult.

*Acknowledgments.* The authors wish to thank Dr. Jing Guo of Drexel University for preparing the ERICA buoy data. This research was supported by the Marine Meteorology Program, Office of Naval Research, Contract N00014-86-K-0203.

#### REFERENCES

- Butler, S. T., 1962: Atmospheric tides. *Sci. Amer.*, **207**, 49–55.  
 Chapman, S., 1951: Atmospheric tides and oscillations. *Compendium*

- of Meteorology, T. F. Malone, Ed., American Meteorological Society, 510–530.  
 —, and R. Lindzen, 1970: *Atmospheric Tides: Thermal and Gravitational*. Gordon and Breach, 200 pp.  
 Forbes, J., and H. Garrett, 1979: Theoretical studies of atmospheric tides. *Rev. Geophys. Space Phys.*, **17**, 1951–1981.  
 Hadlock, R., and C. W. Kreitzberg, 1988: The Experiment on Rapidly Intensifying cyclones over the Atlantic (ERICA) field study: Objectives and plans. *Bull. Amer. Meteor. Soc.*, **69**, 1309–1320.  
 Hamilton, K., 1981: Latent heat release as a possible forcing mechanism for atmospheric tides. *Mon. Wea. Rev.*, **109**, 3–17.  
 Hartnett, E., G. Forbes, and R. Hadlock, 1989: *ERICA Field Phase Summary*, 300 pp. [Available from ERICA Data Center, Dept. of Physics and Atmospheric Science, Drexel University, Philadelphia, PA 19104.]  
 Haurwitz, B., 1964: Atmospheric tides. *Science*, **144**, 1415–1422.  
 Kahler, M., 1989: Effects of nonlinearity on thermal tides in a 3-D numerical model. *J. Atmos. Terr. Phys.*, **51**, 101–110.  
 Kiser, W. L., T. H. Carpenter, and G. W. Brier, 1963: The atmospheric tides at Wake Island. *Mon. Wea. Rev.*, **91**, 566–572.  
 Lindzen, R., 1967: Thermally driven diurnal tide in the atmosphere. *Quart. J. Roy. Met. Soc.*, **93**, 18–42.  
 —, 1978: Effect of daily variations in cumulonimbus activity on the atmospheric semidiurnal tide. *Mon. Wea. Rev.*, **106**, 526–533.  
 Mass, C., W. J. Steenburgh, and D. Schultz, 1991: Diurnal surface-pressure variations over the continental United States and the influence of sea level reduction. *Mon. Wea. Rev.*, **119**, 2814–2830.  
 Rosenthal, S. L., and W. A. Baum, 1956: Diurnal variation of surface pressure over the North Atlantic Ocean. *Mon. Wea. Rev.*, **84**, 379–387.  
 Spar, J., 1952: Characteristics of the semi-diurnal pressure wave in the United States. *Bull. Amer. Meteor. Soc.*, **33**, 438–441.  
 Teitelbaum, H., and F. Vial, 1991: On tidal variability induced by nonlinear interaction with planetary waves. *J. Geophys. Res.*, **96**, 14 169–14 178.  
 —, —, A. Manson, R. Giraldez, and M. Massebeuf, 1989: Nonlinear interaction between the diurnal and semidiurnal tides: Terdiurnal and diurnal secondary waves. *J. Atmos. Terr. Phys.*, **51**, 627–634.  
 Tokioka, T., and I. Yagai, 1987: Atmospheric tides appearing in a global atmospheric general circulation model. *J. Meteor. Soc. Japan*, **65**, 423–438.  
 Tsuda, T., and S. Kato, 1989: Diurnal non-migrating tides excited by a differential heating due to land–sea distribution. *J. Meteor. Soc. Japan*, **67**, 43–54.  
 Zwiers, F., and K. Hamilton, 1986: Simulation of solar tides in the Canadian Climate Centre general circulation model. *J. Geophys. Res.*, **91**, 11 877–11 896.